

# 1 **A New Estimate of Building Floor Space in North America**

2 Jay H. Arehart <sup>a,b\*</sup>, Francesco Pomponi <sup>b</sup>, Bernardino D’Amico<sup>b</sup>, and Wil V. Srubar III<sup>a,c</sup>

3 <sup>a</sup> Department of Civil, Environmental, and Architectural Engineering, University of Colorado Boulder,  
4 ECOT 441 UCB 428, Boulder, Colorado 80309-0428 USA

5 <sup>b</sup> Resource Efficient Built Environment Lab (REBEL), Edinburgh Napier University, Edinburgh, UK

6 <sup>c</sup> Materials Science and Engineering Program, University of Colorado Boulder

7 \* Corresponding Author, E: [jay.arehart@colorado.edu](mailto:jay.arehart@colorado.edu)

8 **Keywords:** floor space, building stock, North America, machine learning

## 9 **Abstract**

10 Floor space is a key variable used to understand the energy and material demands of buildings. Using  
11 recent datasets of building footprints, we employ a random forest regression model to estimate the floor  
12 space of the North American building stock. Our estimate for floor space in 2016 is 88,033 (+15,907 / -  
13 21,861) million m<sup>2</sup>—which is 2.9 times higher than current estimates from national statistics offices. We  
14 also show how floor space per capita (m<sup>2</sup> cap<sup>-1</sup>) is not constant across the North American region,  
15 highlighting the heterogeneous nature of building stocks. As a critical variable in integrated assessment  
16 models to project energy and material demands, this result suggests the following: (1) the North American  
17 building stock is more energy efficient than previously realized, suggesting that buildings are  
18 underutilized, (2) the embodied environmental impacts of buildings have been underestimated in  
19 comparison to operational impacts, and (3) the near-term demand for floor space and, consequently, the  
20 future demand for materials and energy have been largely underestimated.

## 21 **1. Introduction**

22 To meet mid-century targets, the building industry must adapt to reduce greenhouse gas emissions and  
23 limit maximum global temperature rise to less than 1.5 °C. If left unaltered, the construction industry  
24 alone would be responsible for up to 60% of the projected remaining carbon budget of 340 GtCO<sub>2</sub><sup>1</sup>. This

25 presents a challenge, given that the total gross area of the built environment is expected to increase 173%  
26 by 2050 <sup>2</sup>, and buildings will drive a doubling of raw material consumption by 2060 <sup>3</sup>.

27 Many models have been developed to estimate the future resource demand of the global building  
28 stock <sup>4</sup>. These models utilize either “top-down” or “bottom-up” approaches. In “top-down” methods, total  
29 resource consumption (*e.g.*, energy, material) and floor space are known or estimated for the entire  
30 building stock <sup>5</sup>. Useful statistics are then derived and reported per unit area of the total building stock. In  
31 a “bottom-up” approach <sup>6-8</sup>, resource consumption is quantified per unit area (*e.g.*, kWh/m<sup>2</sup>) for specific  
32 building typologies and multiplied by total gross areas of those building typologies within the building  
33 stock to estimate total resource consumption. Regardless of the approach, correct estimates of total  
34 building floor space are critical to ensure accurate quantification of current and future resource demand,  
35 since the results are directly proportional to the magnitude of those estimates. Floor space is typically  
36 estimated by using a floor space per capita for a particular region or per capita income level. Projections  
37 for regional or global floor space are estimated using the appropriate floor space per-capita estimates  
38 scaled by a projected population at specific income levels.

39 Two primary methodologies have been adopted to calculate a floor space per capita. The first  
40 methodology relies on government organizations to collect national-scale data, typically through surveys,  
41 on the number of occupants and building size, which are then aggregated into national-level statistics in a  
42 “top-down” fashion. For example, the Commercial and Residential Energy Consumption Surveys  
43 (CBECS and RECS, respectively) conducted by the US Energy Information Agency (EIA) utilize this  
44 methodology <sup>9</sup> to estimate floor space for both commercial and residential buildings. A similar  
45 methodology, relying on nationally published statistics of building permits issued, estimated that the  
46 residential building stock of the US was 21,846 million m<sup>2</sup> in 2010 <sup>10</sup>. From these estimates of floor  
47 space, floor space per capita are back-calculated (*e.g.*, square-meter of floor space/person or square-meter  
48 of floor space/USD) based upon the total population or gross domestic product (GDP) of the year the  
49 statistics were collected. An example of where this methodology has been applied is in the global-scale

50 EDGE model <sup>6</sup>. This model aggregates data from many national sources, including regions other than  
51 North America, to project regional floor space per capita based upon income levels, resulting in ranges  
52 between 31 m<sup>2</sup> cap<sup>-1</sup> and 111 m<sup>2</sup> cap<sup>-1</sup>. Likewise, another recent estimate of global floor space utilizes a  
53 total per-capita range between 7.56 m<sup>2</sup> cap<sup>-1</sup> and 80.18 m<sup>2</sup> cap<sup>-1</sup> <sup>7</sup>.

54 The second methodology uses surveys of individual buildings to estimate floor space per-capita  
55 metrics for a particular building typology, then aggregating total floor space based upon the total  
56 population. For example, residential net floor space per capita was estimated for the US and Canada to  
57 range between 22.00 m<sup>2</sup> cap<sup>-1</sup> and 50.98 m<sup>2</sup> cap<sup>-1</sup>, depending upon the dwelling type, using a “bottom-up”  
58 modeling approach <sup>11,12</sup>.

59 Each of these methods for calculating per capita floor space has inherent weaknesses. Survey  
60 methods at the regional or national level are not always transparent and may contain implicit or explicit  
61 biases. Likewise, uncertainties in the metrics are not always reported. Additionally, due to the resource  
62 intensity of capturing national-scale data, a limited number of surveys can be performed. For example, the  
63 most recent US EIA RECS surveyed only 5,600 of the estimated 118.2 million dwellings <sup>13</sup>. Another  
64 weakness of all methods is their inability to capture the underutilization of floor space. Surveys of  
65 occupied buildings will fail to capture unoccupied or underutilized building spaces. While capturing  
66 occupied buildings is certainly useful for modeling operational energy demand, it will underestimate the  
67 building stock’s demand for materials and their associated embodied emissions. To date, there has been  
68 no “bottom-up” survey of all North American buildings to quantify total floor space, which is the aim of  
69 this work.

## 70 **2. Aims and Objectives**

71 Floor space estimates underpin many energy and material demand models, yet a single value is commonly  
72 used to estimate the extent of a region’s building stock floor space. These estimates rely on small samples  
73 of the building stock, and so far, have failed to take advantage of recent advances made in deep learning  
74 and image classification. Thus, the present work has three objectives: (1) develop a methodology for

75 using remotely sensed building footprint datasets to estimate total floor space of a building stock, (2)  
76 apply the methodology in the context of the of North American building stock, and (3) report the  
77 uncertainty of floor space per-capita estimates. We define the North America region to include the United  
78 States and Canada to align with the regional definitions used by other models (*e.g.*, International Institute  
79 for Applied Systems Analysis (IIASA) Global Energy Assessment).

### 80 **3. Methodology**

81 Using recently available remotely sensed satellite imagery <sup>14-16</sup>, we propose a new method to estimate  
82 floor space and floor space per capita. This methodology section is divided into subsections to discuss  
83 the datasets, the calculation of geometric features, the machine learning model, validation of the model,  
84 and the limitations.

#### 85 **3.1 Dataset Description and Validation**

86 Three open-source datasets published by Microsoft were used in the analysis to quantify the North  
87 American building stock: (1) US building footprints <sup>14</sup>, (2) Canada building footprints <sup>15</sup>, and (3) US  
88 building footprints with height attributes <sup>16</sup>. The first and second datasets were derived by extracting  
89 building footprints from satellite imagery using deep neural networks, while the third dataset is a subset  
90 of the first with the height attribute determined through interpolation of a digital terrain model.

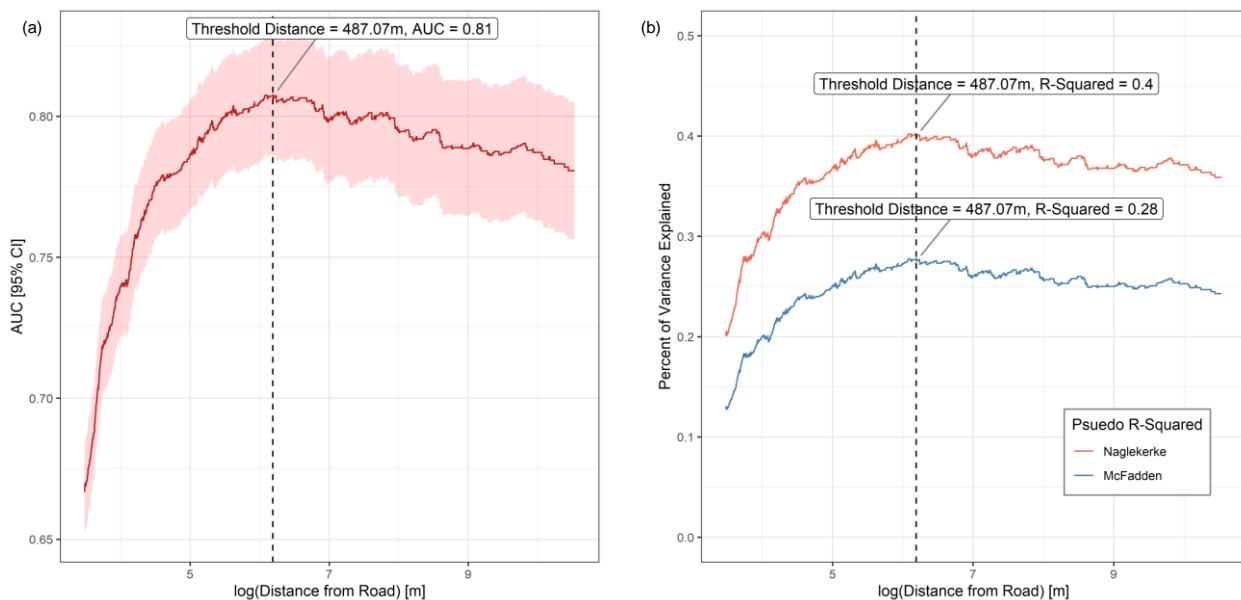
91 The US building footprint dataset was evaluated for its accuracy for three different urban areas  
92 (Los Angeles County, New York City, and Denver) by Heris *et al.*<sup>17</sup>. The authors found it to have  
93 precision (positive prediction value) between 98.2% and 99.5% for these urban areas and recall  
94 (sensitivity) between 93% to 99% for buildings larger than 200m<sup>2</sup>. In addition to the self-reported  
95 accuracy metrics which accompany the published dataset, these additional metrics show that the dataset  
96 accurately identifies true-positives and has very few false positives in urban areas. Yet the Microsoft  
97 building footprint dataset's accuracy has not been assessed rigorously for non-urban areas. Heris *et al.*,  
98 identified many false positives which occurred in areas of open water, high elevation, light colors (*e.g.*,

99 snow and white sand), and bare ground. These false positives often have large footprint areas, making  
100 them problematic for assessing the extent of the North American building stock.

101 To identify and remove these false positives, we perform an analysis under the assumption that  
102 the vast majority of the building stock is located near publicly accessible roads. Thus, the further a  
103 building footprint is from a road, the higher its probability of being a false positive. To do so, we aim to  
104 identify a threshold at which a footprint can be rejected, using logistic regression models. The distance  
105 between a footprint's centroid and nearest road (metric of distance-from-road) is calculated for each  
106 building footprint of the dataset. Datasets for the North American roadways consisted of the US  
107 TIGER/Line shapefiles<sup>18</sup> and Canadian Open Roadway Data<sup>19</sup> which include both paved and unpaved  
108 roads. To ensure sufficient representation of buildings far from roads, we apply a base-10 log-transform  
109 to the distance-from-road metric. We then create a ground-truth dataset to identify the optimal distance-  
110 from-road threshold for which to exclude footprints. To ensure sufficient representation along the tail of  
111 the distribution, and an adequate balance between building and non-building footprints, we sample 150  
112 buildings within each standard deviation of the log-transformed distribution (visualized in **Figure S1.1**).  
113 This sample comprises of 10 sampling buckets ranging from -2SD to +8 SD from the mean. We reviewed  
114 Google satellite imagery for these 1,500 footprints by "hand" to create the ground-truth dataset for which  
115 each building is classified as a building (true positive, *e.g.*, a cabin in a forest), or a non-building (false  
116 positive, *e.g.*, a snow field at high elevation). 408 of the 1,500 footprints (27.2%) are identified to be false  
117 positives, showing sufficient sample size and representation of non-building footprints for the following  
118 logistic-regression models. We use these ground-truth classifications as the outcome variable, and  
119 distance-from-road threshold status (set to 1 if footprint distance-to-road is less than the threshold, and 0  
120 otherwise) as the predictor variable in a series of logistic regression models. Thus, we are able to test the  
121 discriminative ability for a multitude of distance-from-road thresholds, to find which threshold optimally  
122 segregated true building footprints from non-building footprints. We test threshold distances ranging

123 between 32 and 10,000m, and evaluate model accuracy using the area under the receiver-operating  
124 characteristic curve (AUC) and pseudo-R-squared metrics (*i.e.*, Naglekerke and McFadden R-squared).

125 The threshold distance which maximizes the AUC (and most adequately predicted false positives  
126 in the ground-truth dataset) is 487m with an AUC of 0.81. This AUC is considered excellent<sup>20</sup> as the  
127 model at this threshold has an 81% chance of correctly distinguishing true building footprints from non-  
128 building footprints. Across all thresholds, the model with inclusion/exclusion criterion set to 487m  
129 features a global maximum in accuracy as illustrated in **Figure 1** (neither larger nor smaller thresholds  
130 improve the identification of non-building footprints). Thus, filtering on the distance-from-road metric  
131 adequately removes false positives from the dataset. It is important to note that this threshold is  
132 conservative, given that a considerable number of true positives are removed at the expense of filtering  
133 the majority of the less frequent false positives. For instance, large shopping centers surrounded by  
134 parking lots can have a distance from roads greater than 487m and are removed based upon this analysis.  
135 More stringent distance-to-road thresholds have similar model performance ( $AUC_{150m} = 0.77$  and  
136  $AUC_{300m} = 0.80$ ). To be conservative, we utilize a 300m as a threshold for the results presented in **Section**  
137 **4**. Additional results from other threshold distances, both more and less conservative, are included in  
138 **Supplements S5 and S6**.



139

140 **Figure 1. (a)** Area under the ROC curve (AUC) vs. log-transform of the distance from road with 95%  
141 confidence intervals. **(b)** Percent of variance explained using two pseudo R-squared metrics: Naglekerke  
142 and McFadden.

143

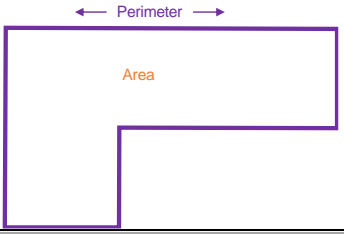
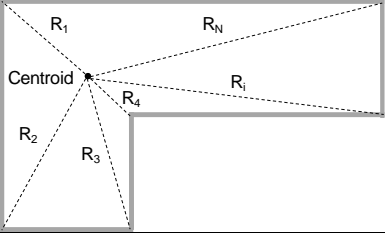
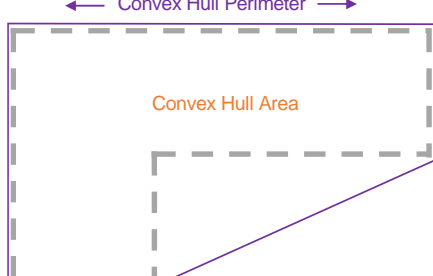
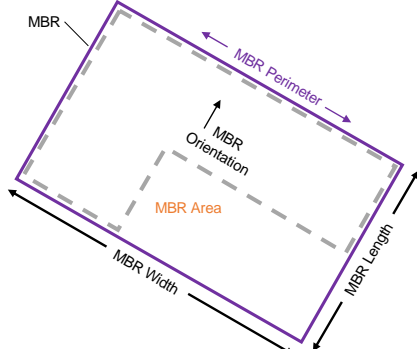
144 The third dataset which we use is a sample of the first dataset and consists of approximately 8  
145 million footprints (6.4% of the total building stock identified by Microsoft) that were captured between  
146 2014 and 2015.<sup>16</sup> The height attribute was determined through the interpolation of a digital terrain model.  
147 This dataset is considered the “training dataset” for the machine learning model and is deemed to be a  
148 representative sample of all buildings in North America. Additional outliers of each dataset are identified  
149 as buildings that are either extremely small, and unlikely to be inhabited (a footprint area smaller than 50  
150 m<sup>2</sup>), or extremely large (a footprint area larger than 10,000 m<sup>2</sup>). Additionally, some outlier data points are  
151 identified in the dataset and removed. For example, the tallest building of the dataset is identified to be a  
152 water tower in Florida with a height of over 9 million meters. This building, and others with obviously  
153 egregious height errors are removed (n=12 of 7,993,302; *i.e.*, 0.00015%), based upon a visual inspection  
154 of the tallest 100 buildings identified in the dataset. Height detection of buildings in urban environments  
155 has typically been limited to the local scales (*i.e.*, cities) and regional and global estimates are a current  
156 focus of the remote sensing community<sup>21</sup>.

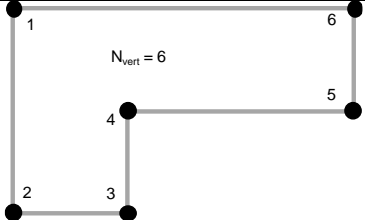
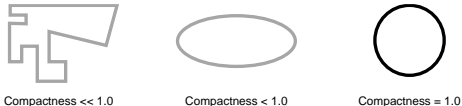
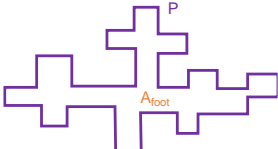
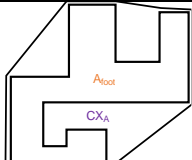
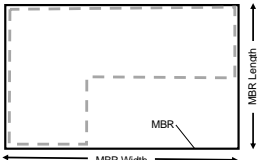
### 157 **3.2 Geometric Features**

158 Each building’s footprint is defined by a GeoJSON string which describes the latitude and longitude of  
159 each of vertex of the footprint. From a building’s footprint geometry, a large number of other metrics can  
160 be derived. We use 19 metrics ranging from the simple (*e.g.*, perimeter and area), to the complex (*e.g.*,  
161 compactness and fractality) as predictor variables for training a machine learning model. The metrics that  
162 are calculated for each building footprint are described in **Table 1**. The calculations are performed under  
163 four geographical projections depending upon the type of calculation (either distance or area) and region  
164 (Canada or United States). For area calculations, we use the USA Continental Equidistant Conic

165 (ESRI:102005) or Canada Albers Equal Area Conic (ESRI:102001) projections, while for distance or  
 166 length calculations, we use the USA Continental Albers Equal Area Conic (ESRI:102003) or Canada  
 167 Lambert Conformal Conic (ESRI:102002) projections.

168 **Table 1.** Description of geometric characteristics of building footprint forms. Each metric is used as a  
 169 predictor variable in the machine learning model which estimates building height.

Variable	Index	Notation or Equation	Description
<b>Size</b>			
	Perimeter	$P$	Perimeter of the footprint.
	Area	$A_{foot}$	Area of the building footprint.
	Mean radius	$R_{mean} = \frac{1}{N} \sum_{i=1}^N R_i$	Mean distance from the building centroid to each vertex of the perimeter.
	Minimum radius	$R_{min} = \min(R_i)$	Minimum distance from the building centroid to each vertex of the perimeter.
	Maximum radius	$R_{max} = \max(R_i)$	Maximum distance from the building centroid to each vertex of the perimeter.
<b>Shape</b>			
	Convex hull perimeter	$CX_p$	Perimeter of the convex hull.
	Convex hull area	$CX_A$	Area of the convex hull.
	Minimum Bounding Rectangle		
	Perimeter	$MBR_p$	Perimeter of the minimum bounding rectangle.
	Area	$MBR_A$	Area of the minimum bounding rectangle.
	Width	$MBR_w$	Width of the minimum bounding rectangle.
	Length	$MBR_l$	Length of the minimum bounding rectangle.
MBR Orientation	$MBR_o$	Orientation of the minimum bounding rectangle (MBR).	

	Number of Vertices	$n_{vert}$	Number of vertices that make up the building footprint geometry.
	Cooke JC index	$\frac{P}{4\sqrt{A_{foot}}} - 1$	Measure of a footprint's shape efficiency with respect to a square <sup>22</sup> .
	Compactness	$\frac{4\pi * A_{foot}}{P^2}$	Measure of a footprint's circularity or compactness <sup>23</sup> .
	Fractality	$1 - \frac{\log(A_{foot})}{2 * \log(P)}$	Logarithmic ratio between the footprint area and perimeter <sup>24</sup> .
	Concavity	$\frac{A_{foot}}{CX_A}$	Ratio of the footprint area to the area of the convex hull <sup>24</sup> .
	Elongation	$\frac{MBR_l}{MBR_w}$	Ratio of the length of the MBR to the width of the MBR <sup>25</sup> .

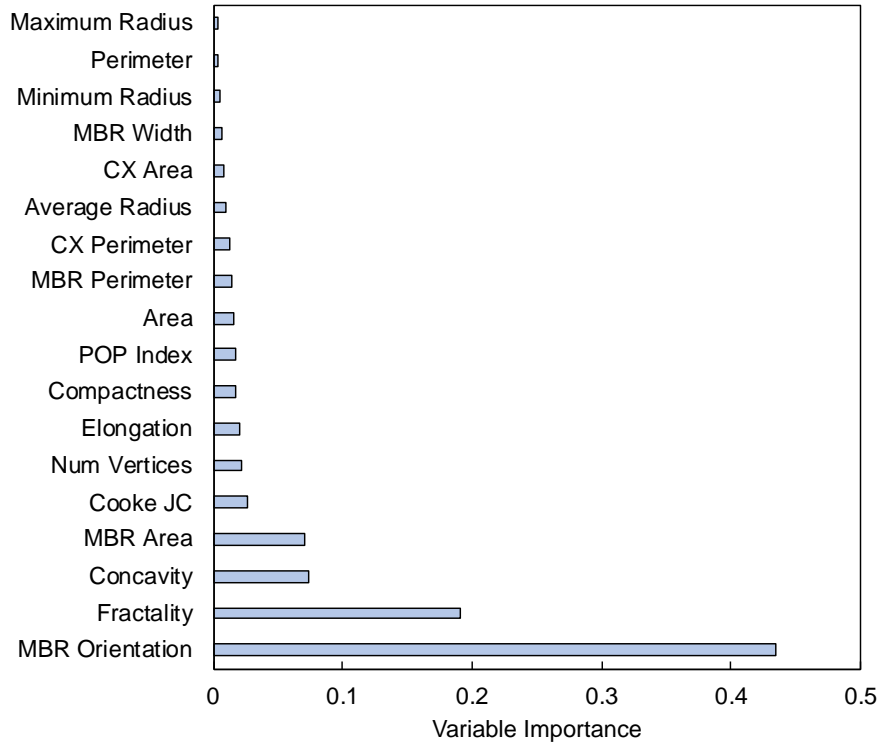
170

### 171 3.3 Machine Learning Model

172 With these predictor variables, the Python scikit-learn (v0.22.1) package <sup>26</sup> is employed to train  
 173 machine learning models. Linear, ridge, support vector machine, gradient boosting, random forest, and  
 174 Adaboost regression models are considered, using a 70/30 training-to-test split of the training dataset.  
 175 Testing mean absolute error (MAE) and model training time are used to evaluate the performance of each  
 176 model. Out of each of the six models, a random forest regression model has the highest performance.  
 177 Random forest regression models are a commonly used ensemble learning method which predict a  
 178 response (in this case building height) based upon the average prediction of many decision trees. A tree is  
 179 formed by creating branches of nodes. Nodes are created at points when the input variables minimize the

180 variance of the response variable. Subsequent nodes are then created along a branch and its length  
181 controlled by the depth of the tree. Controlling the depth of the tree is important to avoid the overfitting of  
182 the model. While useful for high dimension data, random forests are prone to overfitting and are difficult  
183 to visualize, although overfitting can be minimized by tuning the hyperparameters. Upon a large grid  
184 search of hyperparameters with 5-fold cross-validation, the random forest model found to have the lowest  
185 testing MAE consists of 100 trees, makes selections at each node using mean standard error, has a depth  
186 of 10 nodes, is limited to 9 estimators, and for a node to be created requires at least 9 samples. This model  
187 has a training mean absolute error (MAE) of 1.98 m, a training root mean square error (RMSE) of 3.49 m,  
188 a testing MAE of 1.98 m and testing RMSE of 3.52 m. There is negligible difference between the training  
189 and testing MAE suggesting that the identified random forest model is not overfit. This low MAE is a  
190 result of the error of predicting an individual building's height being insignificant in the context of the  
191 entire building stock.

192         While the structure of the forest is difficult to visualize, the predictor variable importance is  
193 summarized in **Figure 2**. Surprisingly, the orientation of the minimum bounding rectangle and fractality  
194 of a building footprint have the most predictive power within the random forest model. We suspect this  
195 result to be attributed to the fact that tall buildings are nearly always located in dense urban areas, while  
196 shorter buildings (*i.e.*, residential buildings) are often located along curved streets in suburbs. In the US  
197 and Canada, many city centers have grid-like road structures oriented along north-south meridians and  
198 east-west circles<sup>27</sup>. Thus, the orientation of the minimum bounding rectangle is useful for separating out  
199 buildings based upon their heights. Likewise, tall buildings are typically simple in their building footprint  
200 and do not consist of multiple wings. Complex building footprints (higher fractality) are often shorter, as  
201 it is less efficient to construct a tall building with a complex footprint. For additional details regarding the  
202 random forest model and predictor variables, see **Supplement S3** for a link to the code and data  
203 repositories.



204

205 **Figure 2.** Variable importance of the predictors used in the random forest regression model.

206

207

208

209

210

This random forest regressor model is applied to all footprints in the US to predict the building height ( $h_i$ ). To quantify uncertainty around each height prediction, the test MAE is added and subtracted to create three height predictions for each building footprint (upper, lower, and predicted). We then estimate the total floor space of North American buildings according to the following:

211

$$F_T = \sum_{i=1}^N A_{foot,i} * \left( \left\lfloor \frac{h_i}{h_{in}} \right\rfloor - 1 \right) \quad (\text{Eq. 1})$$

212

213

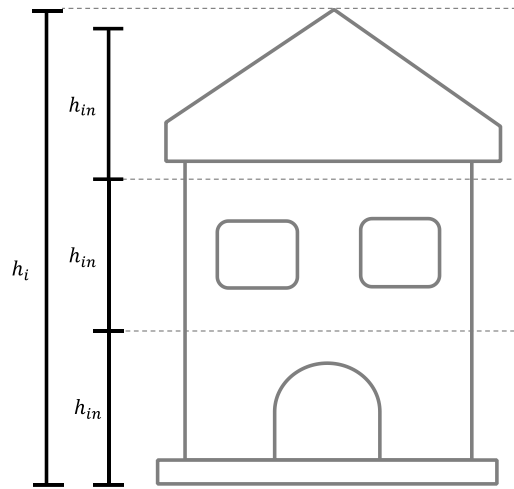
214

215

216

where,  $F_T$  is the total gross floor space,  $A_{foot,i}$  is the individual footprint area,  $h_i$  is the estimated height of each footprint,  $h_{in}$  is the interstory height, and  $N$  is the total number of polygons identified from the satellite imagery.  $h_i$  and  $h_{in}$  are visualized in **Figure 3** for a building with a pitched roof. The number of stories is determined by dividing the estimated height by the interstory height, rounding down to only count full stories, and subtracting one story. For the building in **Figure 3**, Equation 1 calculates the

217 building to have two stories. One story is subtracted due to the height prediction being that of the  
218 maximum height. This value is determined by a visual inspection of the ground truth number of stories of  
219 150 buildings against the predicted number of stories using Google street view imagery<sup>28</sup>. The buildings  
220 sampled are identified in **Supplement S3**. On average, the ground truth number of stories was determined  
221 to be 1.10 stories less than the only using the predicted height since the predicted height is recorded as the  
222 maximum height of the building, rather than the average height.



223

224 **Figure 3.** Visual description of the height variables used by Equation 1.

225

226 A floor space per capita is then estimated by dividing the total floor space by the total population  
227 of each region. It is assumed that the shape of each building is an extrusion of the building footprints and  
228 that only full stories contribute to floor space. This assumption ignores the fact that a building can have  
229 various heights for different parts of its footprint (*e.g.*, a building with wings may have various heights),  
230 or that a façade may be tiered with reduced floor space at higher stories. Because this is a large-scale  
231 regional analysis, and the optimal means of carrying vertical loads is through vertical elements<sup>29</sup>, we  
232 consider the difference in floor space from buildings with discontinuous floor plates to be negligible.  
233 Furthermore, the optimal building form is cuboid in shape, meaning that it is an extrusion from a

234 rectangular shape,<sup>30</sup> yet additional investigation is warranted for determining the extent to which  
235 vertically discontinuous buildings exist in the North American building stock.

### 236 **3.4 Model Validation**

237 To validate the random forest regression model's predictive power, the model is applied to all footprints  
238 in the US building footprints with height attributes<sup>16</sup> dataset. The total floor space is then calculated using  
239 both the reported height (from the training dataset) and predicted height (from the random forest  
240 regression model) with an interstory height of 3.6m. We assume that each building has an interstory  
241 height of 3.6m. This value is determined based upon a sensitivity analysis in which we considered various  
242 distributions of interstory heights. For the details of this sensitivity analysis, see **Supplement S2**. We find  
243 that using a single value of interstory height yields similar results to using other distributions. Interstory  
244 height has not been robustly measured in the North American building stock and would incrementally  
245 improve the present analysis.

### 246 **3.5 Limitations**

- 247 • A key assumption of this analysis is that the training dataset is representative of the entire North  
248 American building stock. While the data is taken from 44 states in the US, it has primarily  
249 coverage of urban areas rather than rural areas. Additionally, the error associated with quantifying  
250 building height using an interpolated digital terrain model is not expressed. While 150 buildings  
251 were visually checked for accurate prediction of number of stories using **Equation 1**, there still  
252 remains some uncertainty with the quality of the building height data used to train the model.
- 253 • Correctly estimating building height is an important component of the model, and this aspect can  
254 be improved upon as new methods for estimating building heights across large scales are  
255 developed<sup>21</sup>. While the quality of the comprehensive building footprint datasets<sup>14,15</sup> were  
256 validated for three metropolitan areas<sup>17</sup>, they have not been validated across the entirety of North  
257 America. Thus, while we manually checked a small fraction of building footprints for their

258 accuracy and deemed them representative, it was not feasible to check the quality of the entire  
259 datasets due to their sheer size.

- 260 • In determining an appropriate distance to road threshold value, only 1500 building footprints  
261 were used. Additional ground-truth sampling of buildings far from roads might refine this  
262 criterion and provide further evidence for the best threshold distance.
- 263 • While the random forest model identified for predicting building heights in this study works well  
264 at the building stock scale, another model may be better suited to predict the height of an  
265 individual building. Furthermore, characteristics other than footprint geometry should be explored  
266 as predictor variables. While the random forest model used had sufficient predictive power for  
267 this study, it may not be the optimal model for predicting individual building heights, which  
268 would be useful for characterizing smaller-scale building stocks.

## 269 **4. Results and Discussion**

### 271 **4.1 Estimate of Floor Space in North America**

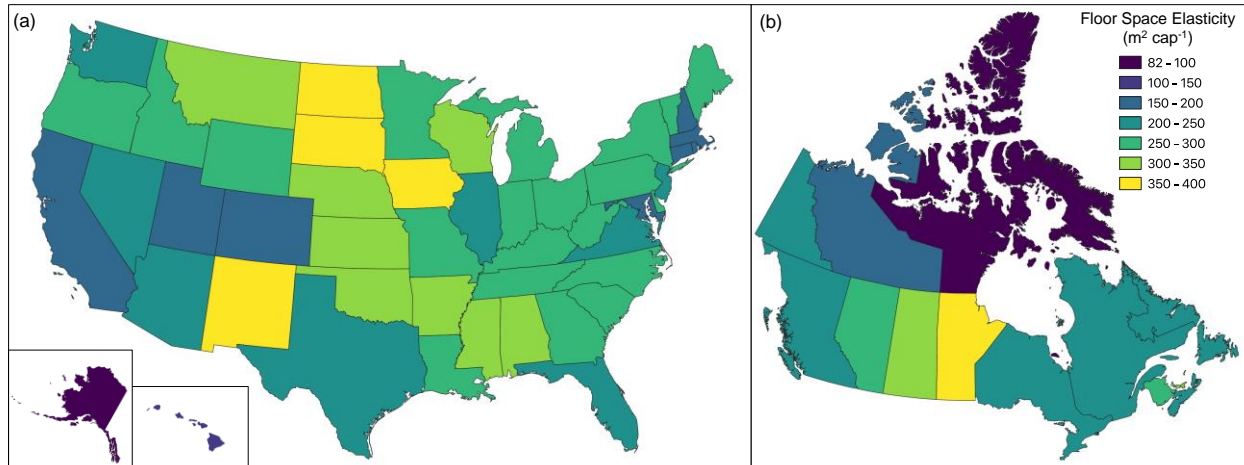
272 Across North America, our model estimates a total of 88,033 million m<sup>2</sup> of floor space with an upper  
273 bound of 103,940 million m<sup>2</sup> and a lower bound of 66,172 million m<sup>2</sup>. Upper and lower estimates are  
274 associated with the error in estimating the height of an individual building footprint (see **Section 3.3**).

275 When converting these estimates to floor space per capita, 242 m<sup>2</sup> cap<sup>-1</sup> is predicted with an upper bound  
276 of 288 m<sup>2</sup> cap<sup>-1</sup> and lower bound of 182 m<sup>2</sup> cap<sup>-1</sup>. The distribution of floor space between the United  
277 States and Canada is 91.6% and 8.4%, respectively. Likewise, there is a 15% difference between the per  
278 capita floor space metrics for the two countries, with the US having 246 m<sup>2</sup> cap<sup>-1</sup> and Canada having 210  
279 m<sup>2</sup> cap<sup>-1</sup>. **Figure 4a** and **4b** show the predicted floor space per capita estimate for each state or territory of  
280 the United States and Canada. Detailed results for these estimates are available in **Supplements 6 and 7**.  
281 No distinction is made herein between residential and non-residential buildings. However, the floor space  
282 could be subsequently disaggregated using high-fidelity data collected from other surveys. For example,

283 the US HAZUS, estimates the US building stock to consist of 77.3% residential, 14.2% commercial, 3.0%  
284 public, and 5.5% agricultural and industrial <sup>31</sup>.

285         The floor space per capita visualized in **Figure 4** show variation between administrative  
286 boundaries. For large-scale models that consider multi-national regions, using an average floor space per  
287 capita is appropriate. However, for sub-national analyses, floor space per-capita estimates vary greatly  
288 between states or territories, and especially, counties. For example, our analysis estimates that Denver  
289 county has a per capita floor space of 141 m<sup>2</sup> cap<sup>-1</sup>, while some rural, sparsely populated counties have  
290 floor space per capita larger than 1000 m<sup>2</sup> cap<sup>-1</sup>. We attribute this result to the large variation in economic  
291 activity between counties, limited land availability driving buildings to be smaller, and the disaggregation  
292 between the location of population centers and the location of buildings. While the metric of floor space  
293 per capita is commonly used for large-scale modeling purposes, caution should be taken when using this  
294 metric for analyses of sub-national building stocks. This analysis' primary aim was to estimate floor space  
295 per capita at the regional scale, so further investigation into individual counties was not performed, yet  
296 may yield interesting insights into the composition and heterogeneity of the North American building  
297 stock.

298         To elucidate whether floor space per-capita metrics are effective means of representing floor  
299 space, the correlation coefficient between population and floor space is computed for all administrative  
300 boundaries. A strong correlation at the state and province level is found (0.976), validating the use of  
301 floor space per capita for prognosticating the future demand and growth of floor space.



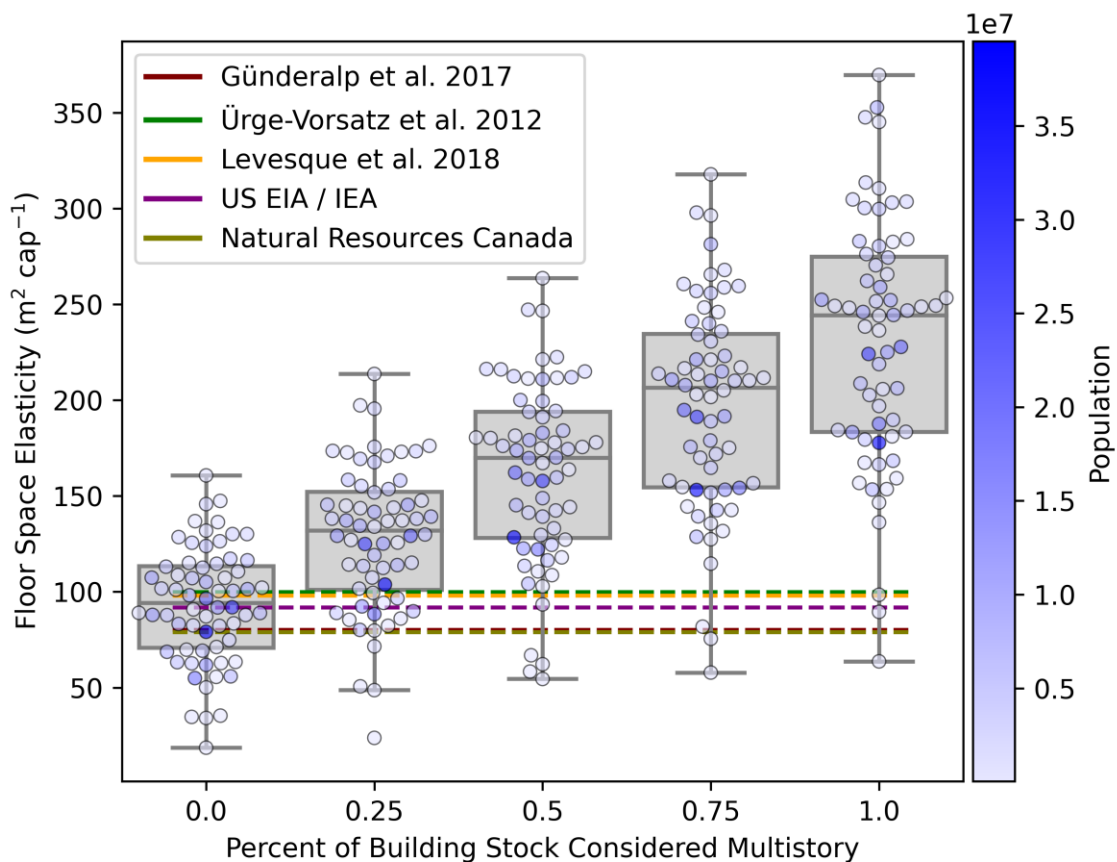
302

303 **Figure 4.** (a) Floor space per capita ( $m^2\ cap^{-1}$ ) for each state in the USA. (b) Floor space per-capita ( $m^2$   
304  $cap^{-1}$ ) for each province and territory of Canada.

#### 305 **4.2 Comparison to Existing Floor Space Estimates**

306 Our estimated floor space per capita are 2.4 – 3.0 times greater than other estimates for the North  
307 American region. As previously discussed, a limiting assumption of our model is that building stock  
308 height data has not been as robustly validated to ground truths as the other building footprint datasets. We  
309 test this assumption by randomly forcing a percentage of the building stock to only be single-story. For  
310 example, a large department store may have a relatively tall building height, yet only be single-story. Our  
311 model would predict it to be a multistory building, when in reality it is only single story. The results of  
312 this analysis are shown in **Figure 5**, with the computed floor space per capita compared against other  
313 estimates<sup>6,7,13,32–34</sup>. Other estimates for floor space align well with one another, often relying on the same  
314 foundational data sets. If we assume the building footprint datasets used herein comprehensively represent  
315 the North American building stock, then to arrive at the floor space per capita used by other models, every  
316 building would be required to be single-story (or 0% considered multi-story). In other words, the total  
317 area of building footprints is equivalent to these other estimates. We know this not to be true, which  
318 demonstrates that these other per-capita floor space metrics drastically and conclusively underestimate the  
319 total floor space in North America.

320 The extent of the underestimation of the North American building stock by many models  
321 necessitates a reevaluation of the methodologies used to estimate floor space per capita. Potential  
322 discrepancies between estimates of per capita floor space may be attributed to buildings being under  
323 occupied, having higher-than-expected rates of unoccupied buildings, or national surveys not being  
324 representative of the total building stock. Moreover, the complexity and uncertainty of commercial floor  
325 space may not be accurately captured by these models.



326  
327 **Figure 5.** Floor space per-capita for different administrative boundaries of the North American building  
328 stock compared against other estimates.

329 **4.3. Implications of Results**

330 Floor space per capita is a critical variable in many global scale models, such as the MESSAGE<sup>35</sup>, EDGE  
331<sup>6</sup>, and TIMER<sup>36</sup> models, which estimate the future energy demand of the building sector. Furthermore,  
332 the demand for construction materials<sup>11,12</sup>, their availability for future reuse<sup>37</sup>, and their potential to store  
333 carbon<sup>38</sup> also rely on this metric, as it is a key driver for projections. These resource demands are modeled  
334 using the Kaya identity methodology<sup>39</sup>. For example, residential energy demand can be modeled as:

$$335 \quad E_{res} = h \frac{p}{h} \frac{A}{p} \frac{E}{A} \quad (\text{Eq. 2})$$

336 where  $E_{res}$  is the total energy demand of a residential building stock,  $h$  is the number of households,  $(p/h)$   
337 is the number of persons per household,  $(A/p)$  is the floor space per capita (or floor space elasticity), and  
338  $(E/A)$  is the energy use intensity for a particular end-use (*e.g.*, space heating or space cooling). A similar  
339 approach can be taken for commercial buildings, using area divided by GDP as the use-intensity driver.  
340 With this modeling approach, the total resource demand of a building stock is directly proportional to the  
341 floor space per capita or floor space per unit of economic output. A second approach uses the floor space  
342 per-capita and simple physics-based models (*e.g.*, degree-day method) or regressions to estimate energy  
343 end-use demand for different building typologies<sup>6</sup>. In both of these approaches, the floor space per-capita  
344 metric is a critical component. While each model which uses the Kaya identity methodology has more  
345 complexity to it than the simple linear relationship presented in **Equation 2**, the total resource demand  
346 estimated by each analysis is directly proportional to the metric of floor space per capita. The results  
347 presented herein cause concern for the estimated resource consumption of the North American building  
348 stock, since the floor space estimates are 2.4 – 3.0 higher than the values used in other modeling efforts.  
349 There may be potential positive sides to this finding. For example, if the current underestimation is a  
350 result of underutilized floor space, then a significant opportunity exists to reduce the demand for new  
351 construction and its associated material and embodied emissions. With more floor space already available  
352 in the building stock, focus can shift from new construction to renovations and refurbishments.

353 Additionally, there is a lack of data that describe building stocks in the Global South. As these  
354 economies continue to develop, it is expected that their floor space per capita will also increase<sup>7,35,40</sup>. This

355 expected increase is based upon estimates for North America and other developed economies. By  
356 underestimating the floor space per capita of higher-income level countries, the current projections for  
357 global floor space growth—especially in the Global South—may be vastly underestimated. This is  
358 concerning given that most of the growth in floor space is expected to occur in the Global South<sup>7</sup>.

359 Bottom-up models for operational energy demand which utilize the Kaya identity methodology  
360 are often validated using top-down estimates. This validation suggests that the floor space per capita used  
361 is appropriately scaled for occupied, conditioned spaces. The results presented by our analysis utilizes a  
362 bottom-up approach, which considers all building footprints in North America, regardless of if they are  
363 unoccupied or unconditioned. To explore this discrepancy, we consider two scenarios. The first is that  
364 operational energy demand is appropriately modeled using floor space per-capita metrics derived from the  
365 US EIA and validated with top-down estimates. When considering the results from our analysis, this  
366 would mean that only up to one-third of the building stock is occupied and conditioned, an implausible  
367 scenario. An alternative scenario is that the building stock is much more energy efficient than previously  
368 realized, due to an extent of underutilization. While some unconditioned buildings (*e.g.*, agricultural and  
369 industrial) are included in our analysis, but excluded in the US EIA’s analysis, they only contribute 5.5%  
370 of the total building stock<sup>31</sup>, which is not enough to rectify the discrepancy observed.

371 Regardless, the fact that the building stock is 2.4 – 3.0 times larger than expected causes concern  
372 when modeling material projections and embodied carbon emissions, since all buildings will have this  
373 demand for material, regardless of whether or not they are fully conditioned. This underestimation of  
374 embodied carbon emissions is worrisome as much of the attention in the past decades has been paid to  
375 reducing operational emissions, when in fact embodied emissions are more significant than realized. By  
376 further characterizing the North American building stock, using bottom-up approaches, we will gain a  
377 better understanding of where the opportunities might lie to reduce life cycle energy demand and carbon  
378 emissions.

379           Understanding floor space per capita is essential to quantifying global resource demand. We  
380 present in this work a novel method for quantifying the floor space of the North American building stock.  
381 The results call for the reevaluation of how floor space per-capita metrics are calculated for building  
382 stocks throughout the world. The methodology for estimating floor space using satellite imagery and  
383 machine learning can be applied to other regions of the world, specifically the Global South, as high-  
384 quality data becomes available. These insights will improve systems-scale models for predicting global  
385 energy and material demand, existing material stocks in the built environment, and the carbon storage  
386 potential of the global building stock. In addition, newfound estimates of floor space per-capita metrics  
387 will aid in identifying and prioritizing building-related interventions required to minimize greenhouse gas  
388 emissions from the building sector.

### 389 **Supporting Information**

390 Details on distance from road threshold; sensitivity analysis of interstory height; link to code repository;  
391 validation of Equation 1; floor space per capita by USA county; additional results for different distance  
392 from road threshold values.

393 **References**

- 394 (1) Müller, D. B.; Liu, G.; Løvik, A. N.; Modaresi, R.; Pauliuk, S.; Steinhoff, F. S.; Brattebø, H. Carbon  
395 Emissions of Infrastructure Development. *Environ. Sci. Technol.* **2013**, *47* (20), 11739–11746.  
396 <https://doi.org/10.1021/es402618m>.
- 397 (2) International Energy Agency. *Transition to Sustainable Buildings: Strategies and Opportunities to*  
398 *2050*; International Energy Agency: Paris, 2013.
- 399 (3) OECD Publishing. *Global Material Resources Outlook to 2060: Economic Drivers and*  
400 *Environmental Consequences*; Paris, 2019.
- 401 (4) Lanau, M.; Liu, G.; Kral, U.; Wiedenhofer, D.; Keijzer, E.; Yu, C.; Ehlert, C. Taking Stock of Built  
402 Environment Stock Studies: Progress and Prospects. *Environ. Sci. Technol.* **2019**, *53* (15), 8499–  
403 8515. <https://doi.org/10.1021/acs.est.8b06652>.
- 404 (5) Schaffartzik, A.; Mayer, A.; Gingrich, S.; Eisenmenger, N.; Loy, C.; Krausmann, F. The Global  
405 Metabolic Transition: Regional Patterns and Trends of Global Material Flows, 1950–2010. *Global*  
406 *Environmental Change* **2014**, *26*, 87–97. <https://doi.org/10.1016/j.gloenvcha.2014.03.013>.
- 407 (6) Levesque, A.; Pietzcker, R. C.; Baumstark, L.; De Stercke, S.; Grübler, A.; Luderer, G. How Much  
408 Energy Will Buildings Consume in 2100? A Global Perspective within a Scenario Framework.  
409 *Energy* **2018**, *148*, 514–527. <https://doi.org/10.1016/j.energy.2018.01.139>.
- 410 (7) Güneralp, B.; Zhou, Y.; Ürge-Vorsatz, D.; Gupta, M.; Yu, S.; Patel, P. L.; Fragkias, M.; Li, X.; Seto,  
411 K. C. Global Scenarios of Urban Density and Its Impacts on Building Energy Use through 2050.  
412 *Proc Natl Acad Sci USA* **2017**, *114* (34), 8945–8950. <https://doi.org/10.1073/pnas.1606035114>.
- 413 (8) Langevin, J.; Harris, C. B.; Reyna, J. L. Assessing the Potential to Reduce U.S. Building CO<sub>2</sub>  
414 Emissions 80% by 2050. *Joule* **2019**, S2542435119303575.  
415 <https://doi.org/10.1016/j.joule.2019.07.013>.
- 416 (9) US EIA. *2015 RECS Square Footage Methodology*; Washington, DC, 2017; p 23.
- 417 (10) Moura, M. C. P.; Smith, S. J.; Belzer, D. B. 120 Years of U.S. Residential Housing Stock and Floor  
418 Space. *PLoS ONE* **2015**, *10* (8), e0134135. <https://doi.org/10.1371/journal.pone.0134135>.
- 419 (11) Marinova, S.; Deetman, S.; van der Voet, E.; Daioglou, V. Global Construction Materials Database  
420 and Stock Analysis of Residential Buildings between 1970-2050. *Journal of Cleaner Production*  
421 **2020**, *247*, 119146. <https://doi.org/10.1016/j.jclepro.2019.119146>.
- 422 (12) Deetman, S.; Marinova, S.; van der Voet, E.; van Vuuren, D. P.; Edelenbosch, O.; Heijungs, R.  
423 Modelling Global Material Stocks and Flows for Residential and Service Sector Buildings towards  
424 2050. *Journal of Cleaner Production* **2019**, 118658. <https://doi.org/10.1016/j.jclepro.2019.118658>.
- 425 (13) US EIA. *Residential Energy Consumption Survey (RECS) - Energy Information Administration*;  
426 2017.
- 427 (14) Microsoft. US Building Footprints. 2018.
- 428 (15) Microsoft. Canadian Building Footprints. 2019.
- 429 (16) Microsoft. Microsoft Buildings Footprint Training Data with Heights. ESRI March 1, 2019.
- 430 (17) Heris, M. P.; Foks, N. L.; Bagstad, K. J.; Troy, A.; Ancona, Z. H. A Rasterized Building Footprint  
431 Dataset for the United States. *Sci Data* **2020**, *7* (1), 207. [https://doi.org/10.1038/s41597-020-0542-](https://doi.org/10.1038/s41597-020-0542-3)  
432 [3](https://doi.org/10.1038/s41597-020-0542-3).
- 433 (18) US Census Bureau. TIGER/Line Shapefiles [https://www.census.gov/geographies/mapping-](https://www.census.gov/geographies/mapping-files/time-series/geo/tiger-line-file.html)  
434 [files/time-series/geo/tiger-line-file.html](https://www.census.gov/geographies/mapping-files/time-series/geo/tiger-line-file.html) (accessed Feb 5, 2020).
- 435 (19) 2016 Census Road Network File - Open Government Portal  
436 <https://open.canada.ca/data/en/dataset/57d5ffae-3048-4a19-9b4c-eab12f6322c5> (accessed Jul 6,  
437 2020).
- 438 (20) Hosmer, D. W.; Lemeshow, S.; Sturdivant, R. X. *Applied Logistic Regression*; John Wiley & Sons,  
439 2013; Vol. 398.

- 440 (21) Li, X.; Zhou, Y.; Gong, P.; Seto, K. C.; Clinton, N. Developing a Method to Estimate Building  
441 Height from Sentinel-1 Data. *Remote Sensing of Environment* **2020**, *240*, 111705.  
442 <https://doi.org/10.1016/j.rse.2020.111705>.
- 443 (22) Kouskoulas, V.; Koehn, E. Predesign Cost-Estimation Function for Buildings. *Journal of the*  
444 *Construction Division* **1974**, *100* (4), 589–604.
- 445 (23) Li, W.; Goodchild, M. F.; Church, R. An Efficient Measure of Compactness for Two-Dimensional  
446 Shapes and Its Application in Regionalization Problems. *International Journal of Geographical*  
447 *Information Science* **2013**, *27* (6), 1227–1250. <https://doi.org/10.1080/13658816.2012.752093>.
- 448 (24) Basaraner, M.; Cetinkaya, S. Performance of Shape Indices and Classification Schemes for  
449 Characterising Perceptual Shape Complexity of Building Footprints in GIS. *International Journal*  
450 *of Geographical Information Science* **2017**, *31* (10), 1952–1977.  
451 <https://doi.org/10.1080/13658816.2017.1346257>.
- 452 (25) Burghardt, D.; Steiniger, S. Usage of Principal Component Analysis in the Process of Automated  
453 Generalisation. In *Proceedings of 22nd international cartographic conference*; 2005; pp 9–16.
- 454 (26) Pedregosa, F.; Varoquaux, G.; Gramfort, A.; Michel, V.; Thirion, B.; Grisel, O.; Blondel, M.;  
455 Prettenhofer, P.; Weiss, R.; Dubourg, V.; Vanderplas, J.; Passos, A.; Cournapeau, D.; Brucher, M.;  
456 Perrot, M.; Duchesnay, E. Scikit-Learn: Machine Learning in Python. *Journal of Machine*  
457 *Learning Research* **2011**, *12*, 2825–2830.
- 458 (27) Boeing, G. Urban Spatial Order: Street Network Orientation, Configuration, and Entropy. *Appl*  
459 *Netw Sci* **2019**, *4* (1), 67. <https://doi.org/10.1007/s41109-019-0189-1>.
- 460 (28) Google. *Google Earth Pro v7.3.3*; Google, 2020.
- 461 (29) Steadman, P. Why Are Most Buildings Rectangular? *Arq* **2006**, *10* (2), 119–130.  
462 <https://doi.org/10.1017/S1359135506000200>.
- 463 (30) D’Amico, B.; Pomponi, F. A Compactness Measure of Sustainable Building Forms. *R. Soc. open*  
464 *sci.* **2019**, *6* (6), 181265. <https://doi.org/10.1098/rsos.181265>.
- 465 (31) FEMA. *HAZUS-MH Software*; US FEMA, 2019.
- 466 (32) Üрге-Vorsatz, D.; Petrichenko, K.; Miklos, M.; Staniec, M.; Labelle, M.; Ozden, E.; Labzina, E.  
467 *Best Practice Policies for Low Energy and Carbon Buildings. A Scenario Analysis*; Center for  
468 Climate Change and Sustainable Policy (3CSEP); Global Buildings Performance Network, 2012.
- 469 (33) IEA; UN Environment Programme. *2018 Global Status Report: Towards a Zero-Emission, Efficient*  
470 *and Resilient Buildings and Construction Sector*; 2018.
- 471 (34) US EIA. *Commercial Building Energy Consumption Survey (CBECS) 2012*; U.S. Energy  
472 Information Administration: Washington, D.C, 2012.
- 473 (35) Grubler, A.; Wilson, C.; Bento, N.; Boza-Kiss, B.; Krey, V.; McCollum, D. L.; Rao, N. D.; Riahi,  
474 K.; Rogelj, J.; De Stercke, S.; Cullen, J.; Frank, S.; Fricko, O.; Guo, F.; Gidden, M.; Havlík, P.;  
475 Huppmann, D.; Kiesewetter, G.; Rafaj, P.; Schoepp, W.; Valin, H. A Low Energy Demand  
476 Scenario for Meeting the 1.5 °C Target and Sustainable Development Goals without Negative  
477 Emission Technologies. *Nat Energy* **2018**, *3* (6), 515–527. [https://doi.org/10.1038/s41560-018-](https://doi.org/10.1038/s41560-018-0172-6)  
478 [0172-6](https://doi.org/10.1038/s41560-018-0172-6).
- 479 (36) Daioglou, V.; van Ruijven, B. J.; van Vuuren, D. P. Model Projections for Household Energy Use in  
480 Developing Countries. *Energy* **2012**, *37* (1), 601–615.  
481 <https://doi.org/10.1016/j.energy.2011.10.044>.
- 482 (37) Stephan, A.; Athanassiadis, A. Towards a More Circular Construction Sector: Estimating and  
483 Spatialising Current and Future Non-Structural Material Replacement Flows to Maintain Urban  
484 Building Stocks. *Resources, Conservation and Recycling* **2018**, *129*, 248–262.  
485 <https://doi.org/10.1016/j.resconrec.2017.09.022>.
- 486 (38) Churkina, G.; Organschi, A.; Reyer, C. P. O.; Ruff, A.; Vinke, K.; Liu, Z.; Reck, B. K.; Graedel, T.  
487 E.; Schellnhuber, H. J. Buildings as a Global Carbon Sink. *Nat Sustain* **2020**, *3* (4), 269–276.  
488 <https://doi.org/10.1038/s41893-019-0462-4>.

- 489 (39) Ürge-Vorsatz, D.; Cabeza, L. F.; Serrano, S.; Barreneche, C.; Petrichenko, K. Heating and Cooling  
490 Energy Trends and Drivers in Buildings. *Renewable and Sustainable Energy Reviews* **2015**, *41*,  
491 85–98. <https://doi.org/10.1016/j.rser.2014.08.039>.  
492 (40) International Energy Agency. *Technology Roadmap Energy Efficient Building Envelopes*; 2013; p  
493 68.  
494

## 495 **Acknowledgments**

496 JA and FP gratefully acknowledge the financial support received for this research by Edinburgh Napier  
497 University, through the project “Carbon Storage of the Built Environment: Exploring the Theoretical  
498 Potential (CaSBE)” - Grant No. N452-000F. Additionally, JA gratefully acknowledges the financial  
499 support from the Temple Hoyne Buell Architectural Fellowship, the College of Engineering’s Global  
500 Enrichment Fund, and the Living Materials Laboratory (LMLab) at the University of Colorado Boulder.  
501 This work represents the views of the authors and not necessarily those of the sponsors. The authors  
502 acknowledge and thank Chris Arehart for his input and insight regarding the methodology for dataset  
503 validation. Additionally, the authors are grateful to the three anonymous referees for their review and  
504 comments that helped improve the clarity and significance of the manuscript.

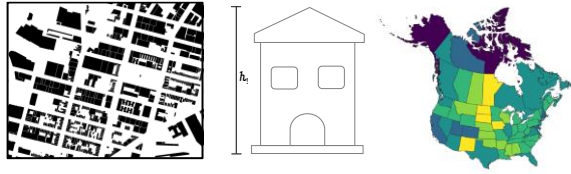
## 505 **Author contributions**

506 All authors conceptualized the research. JA developed the methods and performed the analysis. JA, FP,  
507 and BD contributed to the discussion and interpretation of the results. All authors contributed to the  
508 writing and editing of the manuscript.

## 509 **Competing interests**

510 The authors declare no competing interests.

511 **For Table of Contents Only**



512

